Published in Applied Physics A: Materials Science & Processing 71, issue 7, 615-618, 2000
which should be used for any reference to this work

Oxygen-segregation-controlled epitaxy of Y_2O_3 films on Nb(110)

J. Hayoz*, M. Bovet, T. Pillo, L. Schlapbach, P. Aebi

Institut de physique, Université de Fribourg, Pérolles, 1700 Fribourg, Switzerland

Abstract. We demonstrate a very simple and reliable method of manufacturing clean, single-crystalline Y_2O_3 films on Nb(110) substrates in situ. The method exploits the oxygen bulk contamination of Nb as a source of clean oxygen. For substrate temperatures above 800 K oxygen segregation to the Nb surface is so efficient, that yttrium becomes oxidized during deposition without any background oxygen pressure required in the ultrahigh vacuum system. The crystallinity and stoichiometry of these films can be tuned by the deposition temperature. For Y deposition at 1300 K the formation of well-ordered (111)-oriented Y_2O_3 films is achieved.

PACS: 81.05.Je; 68.55.Jk; 81.15.Ef; 81.65.Mq; 61.14.Hg; 61.14.Qp

Yttria (Y_2O_3) is a highly refractory material that has many practical applications, for example, it is used as sintering aids in the processing of ceramic materials and as a component for rare-earth (RE) doped lasers and optical windows [1]. In the last few years thin yttria films have attracted increasing attention. Its high dielectric constant ($\varepsilon = 13 - 17$), its high resistivity, and high breakdown strength make Y_2O_3 a viable candidate for silicon very-large-scale applications such as high-density storage capacitors in miniaturized dynamic random access memory (DRAM) [2–4]. Moreover, Y_2O_3/Nb tunneling barriers were found among the best in interface quality and the highest in tunneling resistance and, consequently, meet important prerequisites for superconducting digital electronics [2]. It is obvious, that the unique properties of yttria depend critically on the presence of defects. Therefore, a simple and reliable method of manufacturing yttria films with controlled defect concentrations is desirable for both applications as well as for fundamental research on the electronic structure and bonding in crystalline yttria at the microscopic level.

Present address: Departmentof Physics, Pennsylvania State University, PA 16802. (Fax: US-814-865-0978, E-mail: joh4@psu.edu)

Usually, thin Y_2O_3 films are manufactured by evaporation, sputtering, and laser ablation of bulk Y_2O_3 or by postoxidation of Y films in air or oxygen ambient [3–5]. Here we demonstrate a very simple and reliable method of manufacturing clean, single-crystalline Y_2O_3 films on (110)-oriented Nb substrates. Their crystallinity and stoichiometry can be tuned by the deposition temperature. The crystalline quality of the films was examined by means of X-ray photoelectron diffraction (XPD) and low-energy electron diffraction (LEED). X-ray photoelectron spectroscopy (XPS) was used to study the chemical bonding in the yttrium oxide films. Film preparation and characterization were carried out in situ. Angle-resolved ultraviolet photoemission spectroscopy (ARUPS) results on the electronic structure of Y_2O_3 films will be published elsewhere [6].

XPD was chosen because of its chemical sensitivity and its sensitivity to local real-space order. It is a powerful technique for surface structural investigations [7], and it has been shown that full hemispherical XPD patterns provide very direct information about the near-surface structure [8]. At photoelectron kinetic energies above about 500 eV, the strongly anisotropic scattering of photoelectrons by the ion cores leads to a forward-focusing of the electron flux along the emitter-scatterer axis. The photoelectron angular distribution, therefore, is to a first approximation a forward-projected image of the local structure around the photoemitters.

1 Experimental procedures

Experiments were performed in a modified VG ESCALAB Mk II spectrometer (base pressure in the low 10^{-11} mbar region) and equipped with a two-axis sample goniometer enabling sequential computer-controlled sample rotation. Photoelectron spectra and diffraction patterns were measured using Mg K_α ($h\nu = 1253.6$ eV) radiation with the sample kept at room temperature (RT). In the XPD experiments we typically measured about 4500 angle settings ((θ, ϕ), photoelectron emission angles θ(polar) and ϕ(azimuthal)), each displaying the angular-dependent intensity of the selected

core level. The intensities are plotted in so-called diffractograms, i.e., in stereographic projection and in a linear gray scale with maximum intensity corresponding to white (see Fig. 3). In the diffractograms, the outer circle corresponds to grazing emission ($\theta = 90°$) and the center denotes normal emission ($\theta = 0°$).

The Nb(110) substrate was cleaned by cycles of Ar^+-sputtering and annealing until no impurity other than oxygen could be detected with XPS. Oxygen can only be removed from the Nb(110) surface by prolonged heating to 2700 K [9]. In the present study, however, the Nb(110) substrate was never heated above 2000 K. As a result the detected O 1*s* to Nb 3*d* intensity ratio was ≈ 0.35 and LEED displayed a complex pattern. An identical pattern was observed by Franchy et al. [9]. High-purity Y (99.99%) was deposited at different substrate temperatures from a LN_2-cooled electron bombardment evaporation cell at pressures never exceeding 7×10^{-11} mbar. Note, that neither during nor after Y deposition any O_2 background-pressure was applied. The substrate temperature was monitored with an optical pyrometer previously calibrated with a chromel–alumel thermocouple. The thickness of all films was 150 Å as measured by a water-cooled quartz microbalance. Typical deposition rates were 15 Å/min. After Y deposition the Nb 3*d* doublet was no longer detectable, i.e. the Nb(110) substrate was completely covered with Y.

2 Experimental results

Figure 1 displays typical LEED experiments, with the Y film deposited at RT (Fig. 1a), at 700 K (Fig. 1b), at 900 K (Fig. 1c), and at 1300 K (Fig. 1d). LEED from the RT-deposited Y film (Fig. 1a) yields a poorly defined hexagonal pattern, indicative for a low surface order. Below ≈ 800 K the LEED reflexes sharpen and gain in intensity with increasing deposition temperature (Fig. 1b). Additional spots, revealing a structural transition at the surface, are observed for higher deposition temperatures (Fig. 1c,d). As follows from the poorly and well defined LEED pattern of Fig. 1c,d, respectively, a well ordered surface is only achieved when Y is deposited at 1300 K. A careful analysis of the reciprocal surface lattice vectors reveals that the surface periodicity increases by a factor of (4.1±0.1) when going from RT deposition to deposition at 1300 K.

Figure 2 shows the photoemission intensity in the region of the Y 3*d* doublet and the O 1*s* singlet. Com-

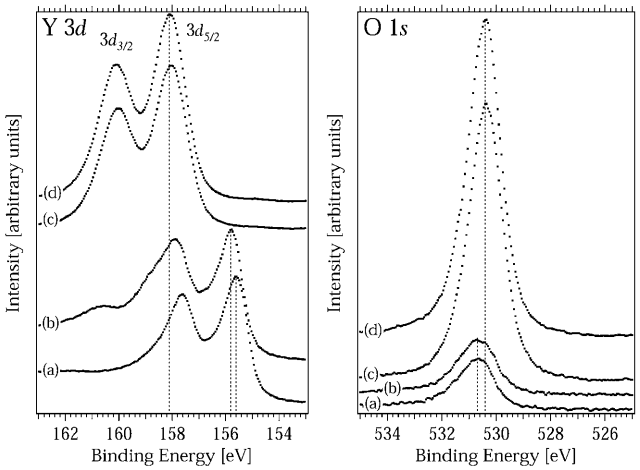

Fig. 2. XPS spectra illustrating peak positions and line shapes of the Y 3*d* doublet and the O 1*s* level respectively, as measured from Y films deposited at different Nb(110) substrate temperatures. (a) RT, (b) 700 K, (c) 900 K, (d) 1300 K

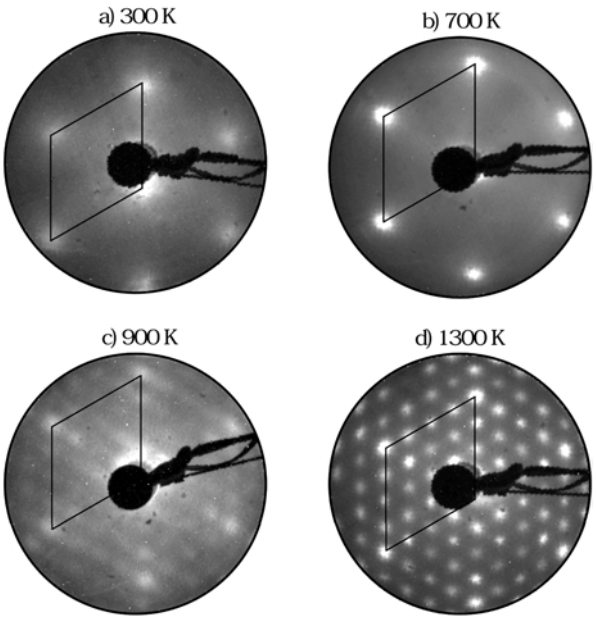

Fig. 1a–d. LEED images ($E_{kin} = 40$ eV) taken from 150 Å thick Y films deposited at different Nb(110) substrate temperatures. **a** RT, **b** 700 K, **c** 900 K, **d** 1300 K. For all images the $[001]_{bcc}$ direction of the underlying Nb(110) crystal is equally oriented to within ±1°. Primitive and (4×4) reciprocal surface unit cells are outlined by rhombohedrons. Note, the rhombohedrons of **c**, **d** are smaller than those of **a**, **b** by a factor of (0.97 ± 0.03)

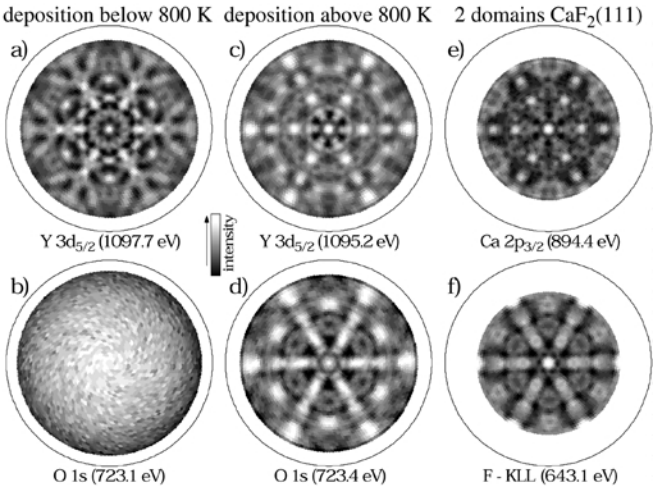

Fig. 3a–f. Stereographic projection of experimental photoelectron intensities. **a** Y $3d_{5/2}$ and **b** O 1*s* intensities from an Y film deposited below ≈ 800 K. **c** Y $3d_{5/2}$ and **d** O 1*s* intensities from an Y film deposited above ≈ 800 K. The patterns **a** – **d** are oriented such that the $[001]_{bcc}$ direction of the underlying Nb(110) crystal points to the top. 2-fold symmetry-averaged **e** Ca $2p_{3/2}$ and **f** F-KLL Auger emission diffractograms taken from a CaF_2 (111) single crystal with the $[10\bar{1}]_{fcc}$ direction pointing to the top. Note that measurements on CaF_2 do not reach as far out in polar angle because of technical reasons (sample mounting)

pared to the spectra taken from Y films deposited at RT (Fig. 2a), the 700 K deposition Y 3*d* doublet is shifted by 0.2 eV towards higher binding energy, whereas the O 1*s* emission line remains almost unmodified. Moreover, the broad Y $3d_{3/2}$ component together with a weak shoulder in the high-binding energy tail of the Y 3*d* doublet indicates the presence of a second Y 3*d* doublet. Most surprisingly, spectra taken from Y films deposited at substrate temperatures above ≈ 800 K (Fig. 2c,d) exhibit a very intense O 1*s* singlet shifted by ≈ 0.3 eV towards lower binding energies. The previously faint second Y 3*d* doublet, which in turn is shifted by 2.5 eV towards higher binding energies, has fully developed and the original Y 3*d* doublet has completely vanished. Note, that for any film no contaminations could be detected with XPS. The change in chemical environment is, therefore, necessarily due to oxide formation.

Obviously, an O-induced phase transformation occurs with increasing deposition temperature at ≈ 800 K. Figure 3 reveals the local structure around the Y and O atoms below and above the transition temperature. The Y $3d_{5/2}$ diffractogram taken from Y films deposited below ≈ 800 K (Fig. 3a) reveals six-fold symmetry. An identical pattern was observed for 150 Å Y deposited at RT at W(110) and was identified as a single-crystalline $hcp(0001)$-oriented Y film [8]. The O 1*s* photoelectron distribution (Fig. 3b) yields a featureless pattern, i.e. for Y films deposited below ≈ 800 K there is no well defined local structure around the O atoms. For Y films deposited above ≈ 800 K, in contrast, XPD reveals local order around both the Y atoms (Fig. 3c) and the O atoms (Fig. 3d).

It is instructive to compare the diffractograms of the high deposition-temperature phase (Fig. 3c,d) with the Ca $2p_{3/2}$ diffractogram (Fig. 3e) and the F-KLL Auger emission pattern (Fig. 3f) of a (111)-oriented CaF_2 single crystal. Note, that the $CaF_2(111)$ diffractograms are averaged for two domains rotated by 180° with respect to each other (see below). For both, emission from the cation sites (Y, Ca) (Fig. 3c,e) and from the anion sites (O, F) (Fig. 3d,f), respectively, the same prominent forward-focusing maxima are observed at identical angles and also the fine structure is very similar [10]. Therefore, the similarity between the local structure around the Y (O) atoms in Y oxide and the local structure around Ca (F) atoms in CaF_2 reveals the formation of two (111)-oriented Y_2O_3 domains rotated by 180° with respect to each other. Indeed, Y_2O_3 is reported to crystallize into the *C*-type RE sesquioxide structure [space group $Ia3-(T_h^7)$], closely related to the fluorite structure [11]. In the fluorite lattice, each cation is surrounded by eight anions located at the corners of a cube. The *C*-type structure is derived by removing one-quarter of the anions and slightly rearranging the remaining ones. This interpretation is consistent with LEED and XPS. The transition from a (1×1) to a (4.1×4.1) surface symmetry (Fig. 1) perfectly agrees with the 4.1-factor between the surface lattice constant of (111)-oriented Y_2O_3 films ($a^{(111)}_{Y_2O_3} = 15.001$ Å) and the basal lattice constant of Y(0001) surfaces ($a^{(0001)}_{Y} = 3.65$ Å). Furthermore, the shift of the Y 3*d* doublet of 2.5 eV towards higher binding energies (Fig. 2) is comparable to bulk values of metallic Y and Y_2O_3 [12].

Principally, the composition of the oxide films in the surface region can be determined from the O 1*s* to Y 3*d* intensity ratio. Its 1.5% increase when going from deposition at 900 K (Fig. 2c) to deposition at 1300 K (Fig. 2c) indicates an increasing O content in the film, i.e. the composition can be tuned by the deposition temperature. However, a reliable quantitative determination of the composition with XPS is difficult. It requires the knowledge of the sample surface termination and of the photoelectron elastic mean free path [13]. Assuming a surface termination with two Y-rich layers facing the vacuum, the experimental O 1*s* to Y 3*d* intensity ratio observed for deposition at 1300 K is consistent with considering a stoichiometric $Y_2O_3(111)$ surface. This, together with the XPD, LEED and core-level shift results, indicates the formation of stoichiometric Y_2O_3 films upon deposition at 1300 K. Furthermore, in agreement with Y_2O_3 stoichiometry, ARUPS reveals a large band-gap without any donor/acceptor subgap states [6].

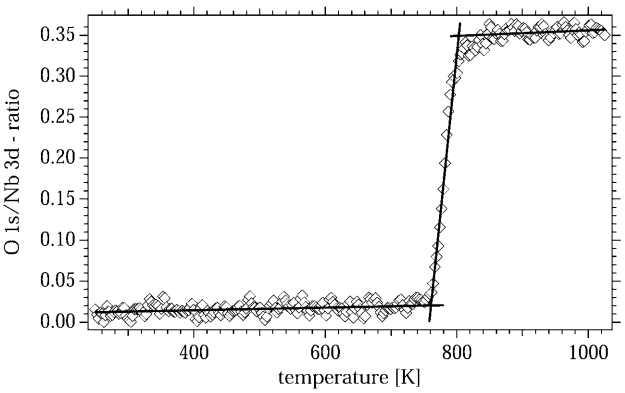

Fig. 4. Behavior of the XPS O 1*s* to Nb 3*d* intensity ratio upon annealing (50 K/min) of an oxygen-free Nb surface (see text). The *solid lines* are linear fits to the data

3 Discussion

Since no oxygen background pressure was applied neither during nor after Y deposition, one may wonder about the provenance of oxygen required to form these Y_2O_3 films. Since for Y deposition on W(110) under equivalent deposition conditions no O contamination is detected [8], oxygen cannot originate from the residual gas. Obviously oxygen disolved in the Nb bulk [14] segregates to the surface and provides a natural source of very clean, atomic oxygen. Then, due to its high reactivity, Y deposited on Nb(110) readily sucks up oxygen. Note that removal of a thick Y_2O_3 film by RT Ar^+ sputtering ends up with a rough, but oxygen-free surface. Obviously, Y deposition above 800 K efficiently depletes the Nb(110) surface region of oxygen. If such an O-depleted Nb(110) surface is annealed (50 K/min), the XPS O 1*s* to Nb 3*d* intensity ratio, remaining almost constant below 760 K, rises steeply to saturation (≈ 0.35) at ≈ 800 K (Fig. 4). Thus, the minimum deposition temperature required to initiate Y_2O_3 formation is determined by the onset of oxygen surface segregation. The formation of well-ordered oxide films, however, requires sufficiently high mass transport, i.e. higher deposition temperature.

4 Conclusion

Exploiting the oxygen bulk contamination of Nb, we have grown clean, single-crystalline $Y_2O_3(111)$ films on Nb(110) in situ. For substrate temperatures above 800 K oxygen segregation to the Nb surface is so efficient, that yttrium becomes oxidized during deposition without any oxygen background pressure required in the ultrahigh vacuum system. The crystallinity and stoichiometry of these films can be tuned by the deposition temperature. For Y deposition at 1300 K the formation of well-ordered and smooth $Y_2O_3(111)$ surfaces is achieved. We would like to point out that oxygen-segregation-controlled epitaxy on Nb(110) is by no means limited to the formation of 150-Å-thick Y_2O_3 films. The 20 to 200 Å regime has been covered successfully [6], and we plan to determine the critical thickness required for the preparation of well-ordered and smooth $Y_2O_3(111)$ films on Nb(110) in future work. Moreover, the deposition of REs, Al, or other reactive elements on Nb(110) above 800 K is expected to yield oxide films of similar quality.

Acknowledgements. Skillful technical assistance was provided by F. Bourqui, C. Neururer, E. Mooser, R. Schmid, and O. Raetzo. This project was supported by the Fonds National Suisse pour la Recherche Scientifique.

References

1. A.A. Kaminskii: In *Laser Crystals* (Springer, Berlin, Heidelberg 1981)
2. M. Gurvitch, L. Manchanda, J.M. Gibson: Appl. Phys. Lett. **51**, 919 (1987)
3. R.N. Sharma, A.C. Rastogi: J. Appl. Phys. **76**, 4215 (1994)
4. J.J. Araiza, M. Cardenas, C. Falcony, V.H. Mendez-Garcia, M. Lopez, G. Contreras-Puente: J. Vac. Sci. Technol. A **16**, 3305 (1998)
5. H. Fukumoto, T. Imura, Y. Osaka: Appl. Phys. Lett. **55**, 360 (1989)
6. J. Hayoz: Ph.D. thesis, University of Fribourg, Switzerland 1999; M. Bovet, J. Hayoz, L. Schlapbach, P. Aebi: to be published TS[a]
7. C.S. Fadley: In *Synchrotron Radiation Research: Advances in Surface Science*, ed. by R.Z. Bachrach, (Plenum Press, New York 1990) Vol. 1
8. J. Hayoz, S. Sarbach, Th. Pillo, E. Boschung, D. Naumović, P. Aebi, L. Schlapbach: Phys. Rev. B **58**, R4270 (1998)
9. R. Franchy, T.U. Bartke, P. Gassmann: Surf. Sci. **366**, 60 (1996)
10. Differences in fine structure and relative intensities in the forward-focusing regime of XPD depend on the emitter–scatterer distance, the atomic type of the scatterer, the wavelength (kinetic electron energy) and on the angular momentum of the outgoing electron wave [see D. Naumović et. al.: Phys. Rev. B **47** 7462 (1993)]. All these parameters are different for Y_2O_3 and CaF_2
11. R.W.G. Wyckoff: In *Crystal Structure*, Chapt. 5 (Intersience, New York 1966)
12. A. Fujimori, L. Schlapbach: J. Phys. C **17**, 341 (1984)
13. The interlayer distance is used to calculate the elastic mean free path of the photoelectrons (see M.P. Seah, W.A. Dench: Surf. Interface Anal. **1**, 2 (1979))
14. Oxygen is dissolved to ≈ 0.1 at % in the Nb bulk (K.H. Rieder, Appl. Surf. Sci., **4**, 183 (1980))